



Published in final edited form as:

J Neuroimaging. 2018 March ; 28(2): 139–149. doi:10.1111/jon.12493.

Neuroimaging of Dilated Perivascular Spaces: From Benign and Pathologic Causes to Mimics

Jeffrey D. Rudie, Andreas M. Rauschecker, Seyed A. Nabavizadeh, and Suyash Mohan

Department of Radiology, Division of Neuroradiology, Perelman School of Medicine at the University of Pennsylvania, Philadelphia, PA.

Abstract

Perivascular spaces (PVSs), also known as Virchow-Robin spaces, are pial-lined, fluid-filled structures found in characteristic locations throughout the brain. They can become abnormally enlarged or dilated and in rare cases can cause hydrocephalus. Dilated PVSs can pose a diagnostic dilemma for radiologists because of their varied appearance, sometimes mimicking more serious entities such as cystic neoplasms, including dysembryoplastic neuroepithelial tumor and multinodular and vacuolating neuronal tumor, or cystic infections including toxoplasmosis and neurocysticercosis. In addition, various pathologic processes, including cryptococcosis and chronic lymphocytic inflammation with pontine perivascular enhancement responsive to steroids, can spread into the brain via PVSs, resulting in characteristic magnetic resonance imaging appearances. This review aims to describe the key imaging characteristics of normal and dilated PVSs, as well as cystic mimics and pathologic processes that directly involve PVSs.

Keywords

Neuroradiology; perivascular spaces; Virchow-Robin spaces

Introduction

Perivascular spaces (PVSs), also known as Virchow-Robin spaces, named after the German pathologist Rudolf Virchow (1821–1902) and French anatomist Charles Philippe Robin (1821–1885) are pial-lined, fluid-filled, structures surrounding the walls of arteries, arterioles, veins, and venules as they course from the subarachnoid space to the brain parenchyma.^{1,2} They do not directly communicate with the subarachnoid space but have been shown to be in continuity with the subpial space.³ Although their precise function is not completely understood, there is evidence that they serve as a lymphatic drainage pathway in the brain playing an immunologic role.⁴ PVSs are believed to be connected in a brain-wide pathway known as the glymphatic system, whereby cerebrospinal fluid (CSF) exchanges with the interstitial fluid within the brain parenchyma, including clearing interstitial solutes such as β -amyloid.⁵

Correspondence: Address correspondence to Jeffrey D. Rudie, MD, PhD, Department of Radiology, University of Pennsylvania, 3400 Spruce St, 1 Founders – MRI Education Center, Philadelphia, PA 19104. Jeffrey.rudie@uphs.upenn.edu.

Conflict of Interest: None.

Methods

All cases presented in this review were obtained from the imaging archives of the University of Pennsylvania Health System between 2007 and 2017 according to IRB #828687 except for the case of mucopolysaccharidosis, which was reproduced from Mohan et al with permission.

Imaging of Perivascular Spaces

Since the advent of high-resolution magnetic resonance imaging (MRI), PVSs have been seen with much higher frequency,⁶ reported in up to 100% of individuals with high-resolution 3-dimensional imaging.⁷ There is some variability in the location and morphology of PVSs seen on MRI. Typically, they are seen as well-defined oval, rounded, or tubular structures with smooth margins.⁸ They are generally seen in clusters, often with a range of different sizes. They are usually bilateral but will often exhibit a somewhat asymmetric in distribution. Normal PVSs are generally smaller than 2 mm in size. Often times, they occur along the path of penetrating arteries. The fluid within a PVS is interstitial fluid. However, the signal intensities of PVSs should be identical to CSF on all sequences. Like CSF, fluid within PVS should fully suppress on Fluid-attenuated inversion recovery (FLAIR) imaging. In addition, they will not display restricted diffusion and will not enhance after contrast administration unless there is a pathologic process spreading into them.

Distribution of Perivascular Spaces

PVSs are characteristically divided into three subtypes based on location⁹ (Fig 1). Type I PVSs appear along lenticulostriate arteries entering the basal ganglia through the anterior-perforated substance (Figs 1A and2). Type II PVSs are found along the path of perforating medullary arteries as they enter cortical gray matter over the high convexities, extending into the white matter (Fig 2B). These spaces often asymmetrically involve one hemisphere. Type III PVSs appear in the midbrain at the pontomesencephalic junction surrounding penetrating branches of the collicular and accessory collicular arteries (Figs 1C and3). However, PVSs can be seen throughout the infra and supratentorial brain wherever vessels are present.

Dilated Perivascular Spaces

A PVS can be considered to be dilated when greater than 5 mm, but atypical morphology consisting of irregular shape has also been used rather than a precise size criteria to classify dilated PVS.^{7,10} The estimated prevalence of dilated PVS is between 1.6% and 3% of healthy individuals.^{7,8} Like normal PVSs, dilated PVSs are also most commonly seen in the basal ganglia, high convexities, and midbrain. However, they can also be seen in other locations throughout the brain including in the cerebellum near the dentate nucleus (Fig 4).

A distinct, fourth category of dilated PVSs has been more recently characterized in the subcortical white matter of the anterior superior temporal lobe. These dilated PVSs often have increased perilesional FLAIR signal, which represents gliosis, and may be mistaken for a cystic neoplasm (Figs 5 and 6).^{11,12} Dilated anterior temporal PVSs can be distinguished from more sinister pathologies by the a lack of clinical symptoms, proximity to

subarachnoid space, identification of adjacent vessels, and stability over time with follow-up imaging.¹¹

Although there is no clear understanding of how PVSs become dilated, there are multiple theories including perivascular myelin loss, fibrosis/obstruction of lymphatic drainage pathways, alterations of arterial wall permeability or ex-vacuo dilation secondary to brain atrophy.⁹ They are seen in people of varying ages, but there is an increased prevalence with advancing age.⁸ Increased amounts of PVSs have also been found in the basal ganglia of patients with vascular dementia compared to Alzheimer's dementia and healthy controls.¹³ This observation is classically described as the "état criblé" pattern,¹⁴ with diffusely prominent PVSs in the basal ganglia (Fig 7). In an experimental hypertensive rat brain model, it was suggested that hypertension increases blood vessel permeability, resulting in perivascular-fluid-induced degeneration of perivascular brain tissue.¹⁵ Dilated PVSs have also been associated with mild traumatic brain injury, thought to reflect early and permanent brain changes.¹⁶ In addition, increased basal ganglia/centrum semiovale PVSs have been associated worse nonverbal reasoning and visuospatial cognitive abilities.¹⁷

Giant Perivascular Spaces

Sometimes PVSs can become markedly dilated, mimicking the appearance of cystic neoplasms. When PVSs are equal to or greater than 1.5 cm (solitary or clusters of multiple contiguous spaces), they are called giant/tumefactive PVSs (aka "cavernous dilatation," or Poirier's Type IIIb "expanding lacunae; Fig 8).^{18–20} Most commonly, these giant PVSs occur in the mesencephalothalamic region, although they can be seen anywhere, including within the frontal lobe (Fig 9). Like dilated anterior temporal PVSs, they may exhibit a small amount of surrounding T2/FLAIR signal abnormality, reflecting gliosis. When in the mesencephalothalamic region, they can cause mass effect on the aqueduct of Sylvius, leading to obstructive hydrocephalus. Hydrocephalus is present in an estimated 43% cases of giant/tumefactive mesencephalothalamic PVS.²⁰ This noncommunicating form of hydrocephalus is usually compensated without findings of transependymal flow, given that the obstruction occurs slowly over a long period of time. Sometimes even mildly dilated PVS, not meeting criteria for giant/tumefactive PVS, can lead to hydrocephalus (Fig 10). In cases where the PVS results in hydrocephalus, treatment with ventriculoperitoneal shunting, cystoperitoneal shunting, or endoscopic third ventriculostomy is indicated.²¹ In addition to the classic appearance of multiple, variably-sized, oval, circumscribed, CSF-filled cysts, PVSs are best distinguished from cystic neoplasms by lack of contrast enhancement and stability in appearance over time.

Pathologic Entities Mimicking and Involving Perivascular Spaces

There is a diverse array of congenital, vascular, infectious, and neoplastic processes with cystic appearances that could be confused with dilated PVSs. In addition, systemic inflammatory, infectious, and neoplastic processes can exhibit a classic pattern of spread through PVSs. Therefore, a better understanding of the typical clinical and imaging appearances of these entities is helpful in distinguishing them from normal and dilated PVS.

Vascular and Inflammatory Insults Mimicking Perivascular Spaces

Chronic vascular or inflammatory insults can mimic dilated PVSs if they occur in areas typically associated with PVSs. Lacunar infarcts, caused by occlusion of penetrating branches of the middle cerebral, posterior cerebral, and basilar arteries may be confused for a PVS in the basal ganglia, thalamus, pons, and periventricular white matter. Although acute and subacute lacunar infarctions are easily distinguished from dilated PVS by the presence of restricted diffusion and mass effect, chronic lacunar infarcts can have a similar appearance to a dilated PVS with a central cystic (encephalomalacic) area. However, chronic lacunar infarcts tend to be slightly larger (often >5 mm), asymmetric, wedge shaped, and exhibit a T2/FLAIR hyperintense rim (Fig 11).²² In addition, cystic periventricular leukomalacia due to pre- or peri-natal hypoxicischemic events can demonstrate cavitory cystic lesions in the periventricular white matter, with loss of white matter volume that can mimic a PVS.²³ However, they are usually seen in premature infants with cerebral palsy; they are associated with T2/FLAIR hyperintensity and may also demonstrate abnormal susceptibility from prior hemorrhage. Similarly, porencephalic cysts, thought to be secondary to a localized cerebral insult during early gestation, can be seen in periventricular white matter.²⁴ In addition to abnormal T2/FLAIR signal, porencephalic cysts also typically communicate with the ventricular system and/or subarachnoid space, helping distinguish them from dilated PVSs. Finally, chronic multiple sclerosis lesions may appear as ovoid CSF filled lesions in the periventricular and juxtacortical white matter.²⁵ As with the other vascular and inflammatory insults, MS plaques are generally distinguished from PVS by surrounding hyperintense T2/FLAIR signal and clinical history.

Benign Cystic Entities Mimicking Perivascular Spaces

Other benign cystic lesions including neuroglial cysts, arachnoid cysts, and neuroenteric cysts can have a similar appearance as dilated PVSs. Neuroglial cysts, also called gliependymal cysts, are benign epithelial-lined lesions that can be found anywhere along the neuroaxis.²⁶ Intraparenchymal neuroglial cysts, which are more common than extraparenchymal neuroglial cysts, are congenital lesions arising from embryonic neural tube elements sequestered in the developing white matter (Fig 12).²⁷ Neuroglial cysts do not communicate with the ventricular system or arachnoid space, but are solitary lesions, distinguishing them from PVS.²⁶ Arachnoid cysts are thought to be diverticula emanating from septations of arachnoid membranes, connected to the subarachnoid space.²⁸ Arachnoid cysts are fairly easily distinguished from PVS as they are extraaxial CSF fluid collections, commonly seen in the middle cranial fossa and perisellar cisterns.²⁹ Neuroenteric cysts are congenital endodermal lesions, a rare type of foregut duplication cyst.³⁰ They are most often seen in the posterior fossa and spine, and are often hyperintense on T1 and FLAIR due to proteinaceous contents. Finally, choroidal cysts, seen at the level of the choroidal fissure, can be arachnoid or neuroepithelial in nature.³¹ They will also be solitary, but otherwise can have a similar appearance as a dilated PVS. Although these benign cystic entities share many imaging features with dilated PVSs and are also usually seen incidentally, the key features in distinguishing them is based on their location and that they are usually solitary compared with PVSs which come in clusters.

Neoplastic Cystic Entities Mimicking Perivascular Spaces

A variety of low-grade cystic neoplasms can mimic the appearance of dilated PVSs. Most cystic brain tumors, such as pilocytic astrocytomas, gangliogliomas, and pleomorphic xanthoastrocytomas, are fairly easily distinguished from enlarged PVSs as they will generally contain solid components with enhancement, restricted or facilitated diffusion and surrounding edema/T2/FLAIR signal abnormality. Dysembryoplastic neuroepithelial tumors (DNETs) and multinodular and vacuolating neuronal tumors (MVNTs) could possibly be mistaken for dilated PVSs. DNETs are benign, slow growing WHO grade I tumors classically involving medial temporal lobes and causing complex partial seizures.³² They have a characteristic “bubbly” cystic appearance with fairly extensive associated T2/FLAIR signal abnormality and minimal enhancement in 20–30% of cases (Fig 13).³³ MVNT is a more recently characterized benign, mixed glial neuronal lesion consisting of a subcortical cluster of tiny, cystic, nodular lesions with associated T2/FLAIR signal abnormality (Fig 14).^{34–36} MVNTs are usually seen in the deep cortical ribbon and superficial subcortical white matter in the high convexities.³⁵ They are associated with seizures in around 30% of patients and rarely show progression or enhancement.³⁶

Infectious Cystic Entities Mimicking Perivascular Spaces

Rare infectious processes can also lead to multiple cystic lesions in the brain. Neurocysticercosis, caused by the pork tapeworm *Taenia solium*, is the most common parasitic infection in the central nervous system (CNS) and the most common cause of acquired epilepsy worldwide.³⁷ Initial infections appear as somewhat simple cystic lesions at the gray-white junction and basal ganglia, resembling a dilated PVS, but as they progress through colloidal, granular, and nodular stages, the fluid becomes hyperintense with rim enhancement and surrounding edema, with the lesions eventually becoming shrunken with calcifications.³⁸ Neurotoxoplasmosis is an opportunistic infection most often seen in immunocompromised patients with HIV. Cats are its definitive host and it classically spreads through exposure to cat feces.³⁹ Typically, cerebral toxoplasmosis is characterized by multiple peripherally or ring enhancing lesions, with a “target sign” within the basal ganglia, corticomedullary junction, sometimes with intrinsic T1 shortening and/or susceptibility (Fig 15).⁴⁰

Pathologic Entities Directly Involving Perivascular Spaces

Systemic infectious, inflammatory, metabolic, and neoplastic processes can also show a direct pattern of spread through PVSs. Cryptococcosis is an opportunistic fungal infection caused by *Cryptococcus neoformans*, also most commonly seen in HIV patients. The infection can have a meningeal or parenchymal pattern of spread through the CNS, the latter being associated with infection along the PVS, which can become distended with mucoid, gelatinous material, displaying hyperintense FLAIR signal, and sometimes restricted diffusion or contrast enhancement (Fig 16).⁴¹ CNS involvement is seen in 15% of patients with sarcoidosis, a multisystem granulomatous autoimmune process to an unknown antigen.⁴² Neurosarcoidosis can exhibit meningeal spread extending into the parenchyma along the PVSs with leptomeningeal enhancement (Fig 17), or can manifest as dural thickening or parenchymal masses.⁴³ Intravascular lymphoma is a rare, systemic extranodal large B-cell

lymphoma that proliferates within the lumen of small- to medium-sized blood vessels, demonstrating CNS involvement in 15% of cases, also characterized by leptomeningeal enhancement along the PVSs in the basal ganglia and midbrain (Fig 18).^{44,45} A recently described uncommon entity known as “chronic lymphocytic inflammation with pontine perivascular enhancement responsive to steroids” (CLIPPERS) is characterized by infiltration of inflammatory cells along the PVSs in the pons and brainstem (Fig 19).⁴⁶ The etiology of CLIPPERS is unknown. It has a relapsing-remitting course, responds to high-dose corticosteroids or immunosuppressive treatments, and can lead to hindbrain atrophy.⁴⁷ Finally, inherited disorders of metabolism, such as mucopolysaccharidoses, can cause toxic metabolites accumulate within PVSs, causing dilation and associated surrounding T2/FLAIR signal abnormality (Fig 20).⁴⁸

Conclusion

PVSs demonstrate variable, yet characteristic imaging and spatial patterns, allowing them to be distinguished from an array of infectious, inflammatory, and neoplastic processes that can mimic their appearance or exhibit a pattern of spread along their distribution. Typically, they are seen as clusters of variably sized cystic lesions, exhibiting CSF signal across all sequences. They should not enhance, display abnormal restricted diffusion, or exhibit any T2/FLAIR signal abnormalities. Notable exceptions include giant/tumefactive PVS, most commonly seen in the mesencephalothalamic region, as well as dilated anterior temporal PVS, both of which may demonstrate some T2/FLAIR signal abnormality but should remain stable over time. Understanding these characteristic imaging findings of PVS and more sinister pathologic entities is important for accurate diagnosis and avoidance of unnecessary invasive diagnostic procedures or treatments. Although distinguishing dilated PVS from their mimics is usually straightforward when based on these clinical and imaging characteristic, sometimes, the initial diagnosis may remain ambiguous, and in these cases, close serial follow-up should be performed.

References

1. Virchow R Ueber die erweiterung kleinerer gefaesse. *Arch Pathol Anat Physiol Klin Med* 1851;3:427–62.
2. Robin C Recherches sur quelques particularites de la structure des capillaires de l'encephale. *J Physiol Homme Animaux* 1859;2:537–48.
3. Zhang ET, Inman CB, Weller RO. Interrelation-ship of the pia mater and the perivascular (Virchow-Robin) spaces in the human cerebrum. *J Anat* 1990;170:111–23. [PubMed: 2254158]
4. Schley D, Carare-Nnadi R, Please CP, et al. Mechanisms to explain the reverse perivascular transport of solutes out of the brain. *J Theor Biol* 2006;238:962–74. [PubMed: 16112683]
5. Iliff JJ, Wang M, Liao Y, et al. A paravascular pathway facilitates CSF flow through the brain parenchyma and the clearance of interstitial solutes, including amyloid β . *Sci Trans Med* 2012;4:01–11.
6. Oztürk MH, Aydingöz U. Comparison of MR signal intensities of cerebral perivascular (virchow-robin) and subarachnoid spaces. *J Comput Assist Tomogr* 2002;26:902–4. [PubMed: 12488733]
7. Groeschel S, Chong WK, Surtees R, et al. Virchow-Robin spaces on magnetic resonance images: Normative data, their dilatation, and a review of the literature. *Neuroradiology* 2006;48:745–54. [PubMed: 16896908]
8. Heier LA, Bauer CJ, Schwartz L, et al. Large Virchow-Robin spaces: MR-clinical correlation. *AJNR Am J Neuroradiol* 1989;10:929–36. [PubMed: 2505536]

9. Kwee RM, Kwee TC. Virchow-Robin spaces at MR imaging. *Radiographics* 2007;27:1071–86. [PubMed: 17620468]
10. Mohan S, Verma A, Sitoh YY, et al. Virchow-Robin spaces in health and disease. *Neuroradiology J* 2009;22:518–24.
11. Rawal S, Croul SE, Willinsky RA, et al. Subcortical cystic lesions within the anterior superior temporal gyrus: A newly recognized characteristic location for dilated perivascular spaces. *AJNR Am J Neuroradiol* 2014;35:317–22. [PubMed: 23945225]
12. Lim AT, Chandra RV, Trost NM, et al. Large anterior temporal Virchow-Robin spaces: Unique MR imaging features. *Neuroradiology* 2015;57:491–9. [PubMed: 25614333]
13. Hansen TP, Cain J, Thomas O, et al. Dilated perivascular spaces in the basal ganglia are a biomarker of small-vessel disease in a very elderly population with dementia. *AJNR Am J Neuroradiol* 2015;36:893–8. [PubMed: 25698626]
14. Román GC. On the history of lacunes, État criblé, and the white matter lesions of vascular dementia. *Cerebrovasc Dis* 2002;12:1–6.
15. Suzuki K, Masawa N, Takatama. Pathogenesis of état criblé in experimental hypertensive rats. *J Stroke Cerebrovasc Dis* 2011;10:106–12.
16. Inglese M, Bomsztyk E, Gonen O, et al. Dilated perivascular spaces: Hallmarks of mild traumatic brain injury. *AJNR Am J Neuroradiol* 2005;26:719–24. [PubMed: 15814911]
17. MacLulich AM, Wardlaw JM, Ferguson KJ, et al. Enlarged perivascular spaces are associated with cognitive function in healthy elderly men. *J Neurol Neurosurg Psychiatry* 2004;75:1519–23. [PubMed: 15489380]
18. Kanamalla US, Calabro F, Jinkins JR. Cavernous dilatation of mesencephalic Virchow-Robin spaces with obstructive hydrocephalus. *Neuroradiology* 2000;42:881–4. [PubMed: 11198205]
19. Poirier J, Barbizet J, Gaston A. Thalamic dementia. Expansive lacunae of the thalamo-paramedian mesencephalic area. Hydrocephalus caused by stenosis of the aqueduct of Sylvius. *Rev Neurol (Paris)* 1983;139:349–58. [PubMed: 6137053]
20. Salzman KL, Osborn AG, House P, et al. Giant tumefactive perivascular spaces. *AJNR Am J Neuroradiol* 2005;26:298–305. [PubMed: 15709127]
21. Smith KA, Lavin P, Chamoun R. Neuroendoscopic treatment of symptomatic giant Virchow-Robin spaces. *Surg Neurol Int* 2015;6:120. [PubMed: 26257981]
22. Bokura H, Kobayashi S, Yamaguchi S. Distinguishing silent lacunar infarction from enlarged Virchow-Robin spaces: A magnetic resonance imaging and pathological study. *J Neurol* 1998;245:116–22. [PubMed: 9507419]
23. Hinojosa-Rodriguez M, Harmony T, Carillo-Prado C, et al. Clinical neuroimaging in the preterm infant: Diagnosis and prognosis. *Neuroimage Clin* 2017;16:355–68. [PubMed: 28861337]
24. Abergel A, Lacalm A, Massoud M, et al. Expanding porencephalic cysts: Prenatal imaging and differential diagnosis. *Fetal Diagn Ther* 2017;41:224–33.
25. Sarbu N, Shih RY, Jones RV, et al. White matter diseases with radiologic-pathologic correlation. *Radiographics* 2016;36:1426–47. [PubMed: 27618323]
26. Osborn AG, Preece MT. Intracranial cysts: Radiologic-pathologic correlation and imaging approach. *Radiology* 2006;239:650–64. [PubMed: 16714456]
27. Epelman M, Daneman A, Blaser SI, et al. Differential diagnosis of intracranial cystic lesions at head US: Correlation with CT and MR imaging. *Radiographics* 2006;26:173–96. [PubMed: 16418251]
28. Al-Holou WN, Terman S, Kilburg C, et al. Prevalence and natural history of arachnoid cysts in adults. *J Neurosurg* 2013;118:222–31. [PubMed: 23140149]
29. Keersmaecker BD, Ramaekers P, Claus F, et al. Outcome of 12 antenatally diagnosed fetal arachnoid cysts: Case series and review of the literature. *Eur J Paediatr Neurol* 2015;19:114–21. [PubMed: 25599983]
30. Preece MT, Osborn AG, Chin SS, et al. Intracranial neurenteric cysts: Imaging and pathology spectrum. *AJNR Am J Neuroradiol* 2006;27:1211–6. [PubMed: 16775266]

31. de Jong L, Thewissen L, van Loon J, et al. Choroidal fissure cerebrospinal fluid-containing cysts: Case series, anatomical consideration and review of the literature. *World Neurosurg* 2011;75:704–8. [PubMed: 21704940]
32. Campos AR, Clusmann H, von Lehe M, et al. Simple and complex dysembryoplastic neuroepithelial tumors (DNT) variants: Clinical profile, MRI, and histopathology. *Neuroradiology* 2009;51:433–43. [PubMed: 19242688]
33. Fernandez C, Girard N, Paz Paredes A, et al. The usefulness of MR imaging in the diagnosis of dysembryoplastic neuroepithelial tumor in children: A study of 14 cases. *AJMR Am J Neuroradiol* 2003;24:829–34.
34. Nunes RH, Hsu CC, da Rocha AJ, et al. Multinodular and vacuolating neuronal tumor of the cerebrum: A new “leave me alone” lesion with a characteristic imaging pattern. *AJNR Am J Neuroradiol* 2017;38:1899–904. [PubMed: 28705817]
35. Alsufayan R, Alcaide-Leon P, de Tilly LN, et al. Natural history of lesions with the MR imaging appearance of multinodular and vacuolating neuronal tumor. *Neuroradiology* 2017;59:873–83. [PubMed: 28752311]
36. Huse JT, Edgar M, Halliday J, et al. Multinodular and vacuolating neuronal tumors of the cerebrum: 10 cases of a distinctive seizure-associated lesion. *Brain Pathol* 2013;23:515–24. [PubMed: 23324039]
37. Reddy DS, Volkmer R. Neurocysticercosis as an infectious acquired epilepsy worldwide. *Seizure* 2017;52:176–81. [PubMed: 29055271]
38. Venkat B, Aggarwal N, Makhaik S, et al. A comprehensive review of imaging findings in human cysticercosis. *Jpn J Radiol* 2016;34:241–57. [PubMed: 26903229]
39. Chang L, Cornford ME, Chiang FL. Radiologic-pathologic correlation. Cerebral toxoplasmosis and lymphoma in AIDS. *AJNR Am J Neuroradiol* 1995;16:1653–63. [PubMed: 7502971]
40. Masamed R, Meleis A, Lee EW, et al. Cerebral toxoplasmosis: Case review and description of a new imaging sign. *Clin Radiol* 2009;64:560–3. [PubMed: 19348854]
41. Starkey J, Miritani T, Kirby P. MRI of CNS fungal infections: Review of aspergillosis to histoplasmosis and everything in between. *Clin Neuroradiol* 2014;24:217–30. [PubMed: 24870817]
42. Gascón-Bayarri J, Mañá J, Martínez-Yélamos S, et al. Neurosarcoidosis: Report of 30 cases and a literature survey. *Eur J Intern Med* 2011;22:125–32. [PubMed: 21402241]
43. Nozaki K, Judson MA. Neurosarcoidosis: Clinical manifestations, diagnosis and treatment. *Presse Med* 2012;41:331–48.
44. Yamamoto A, Kikuchi Y, Homma K, et al. Characteristics of intravascular large B-cell lymphoma on cerebral MR imaging. *AJNR Am J Neuroradiol* 2012;33:292–6. [PubMed: 22173763]
45. Fonkem E, Dayawansa S, Stroberg E, et al. Neurological presentations of intravascular lymphoma (IVL): Meta-analysis of 654 patients. *BMC Neurol* 2016;16:9. [PubMed: 26849888]
46. Pittock SJ, Debruyne J, Krecke KN, et al. Chronic lymphocytic inflammation with pontine perivascular enhancement responsive to steroids (CLIPPERS). *Brain* 2010;133:2626–34. [PubMed: 20639547]
47. Taieb G, Allou T, Labauge P. Therapeutic approaches in CLIPPERS. *Curr Treat Options Neurol* 2017;19:17. [PubMed: 28386850]
48. Matheus MG, Castillo M, Smith JK, et al. Brain MRI findings in patients with mucopolysaccharidosis types I and II and mild clinical presentation. *Neuroradiology* 2004;46:666–72. [PubMed: 15205860]

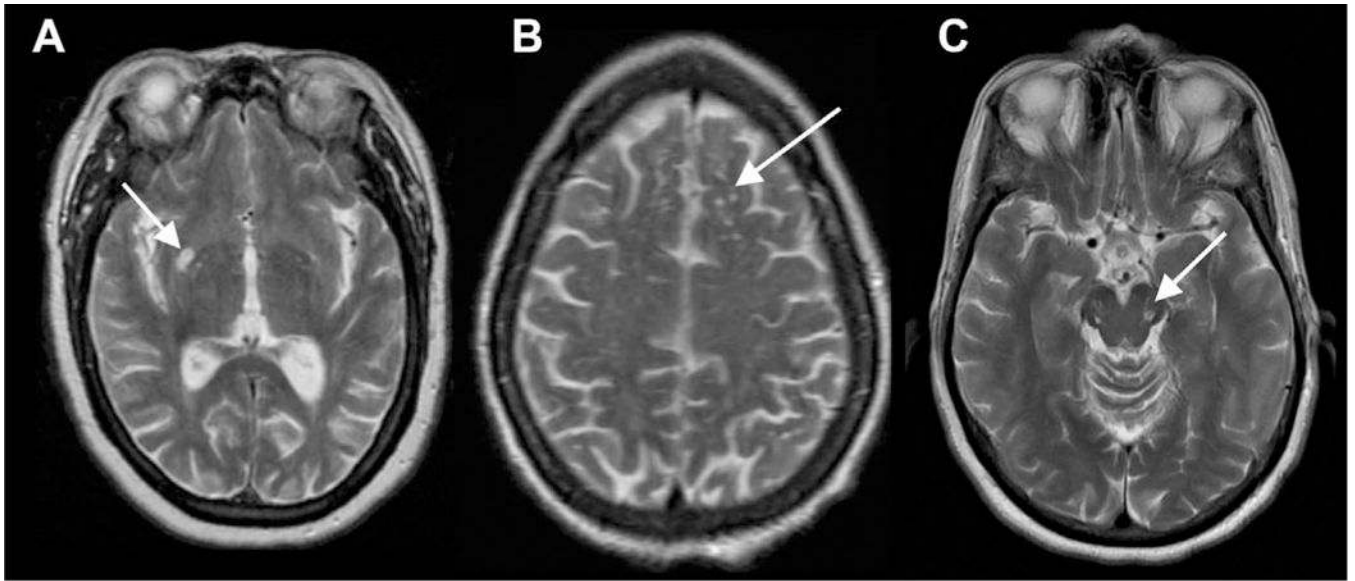


Fig 1. Characteristic locations of PVSs seen on T2 MR images. Type I: basal ganglia along the course of lenticulostriate arteries (A). Type II: subcortical white matter in the high convexities (B). Type III: midbrain at the pontomesencephalic junction (C).

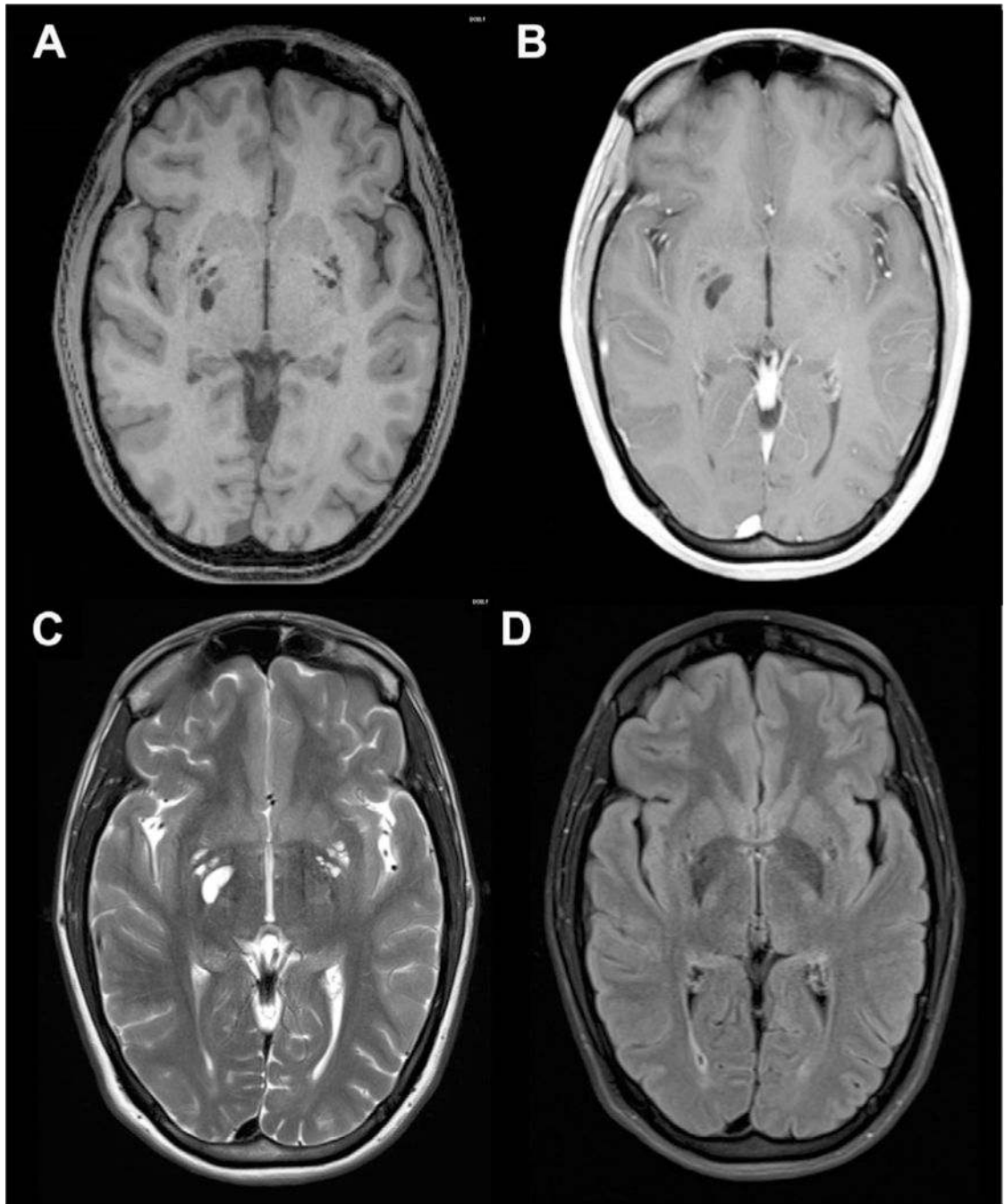


Fig 2. Dilated PVSs in the right greater than left basal ganglia. The PVSs are isointense to CSF on T1 (A), T1 postcontrast (B), T2 (C), and FLAIR (D) axial MR images.

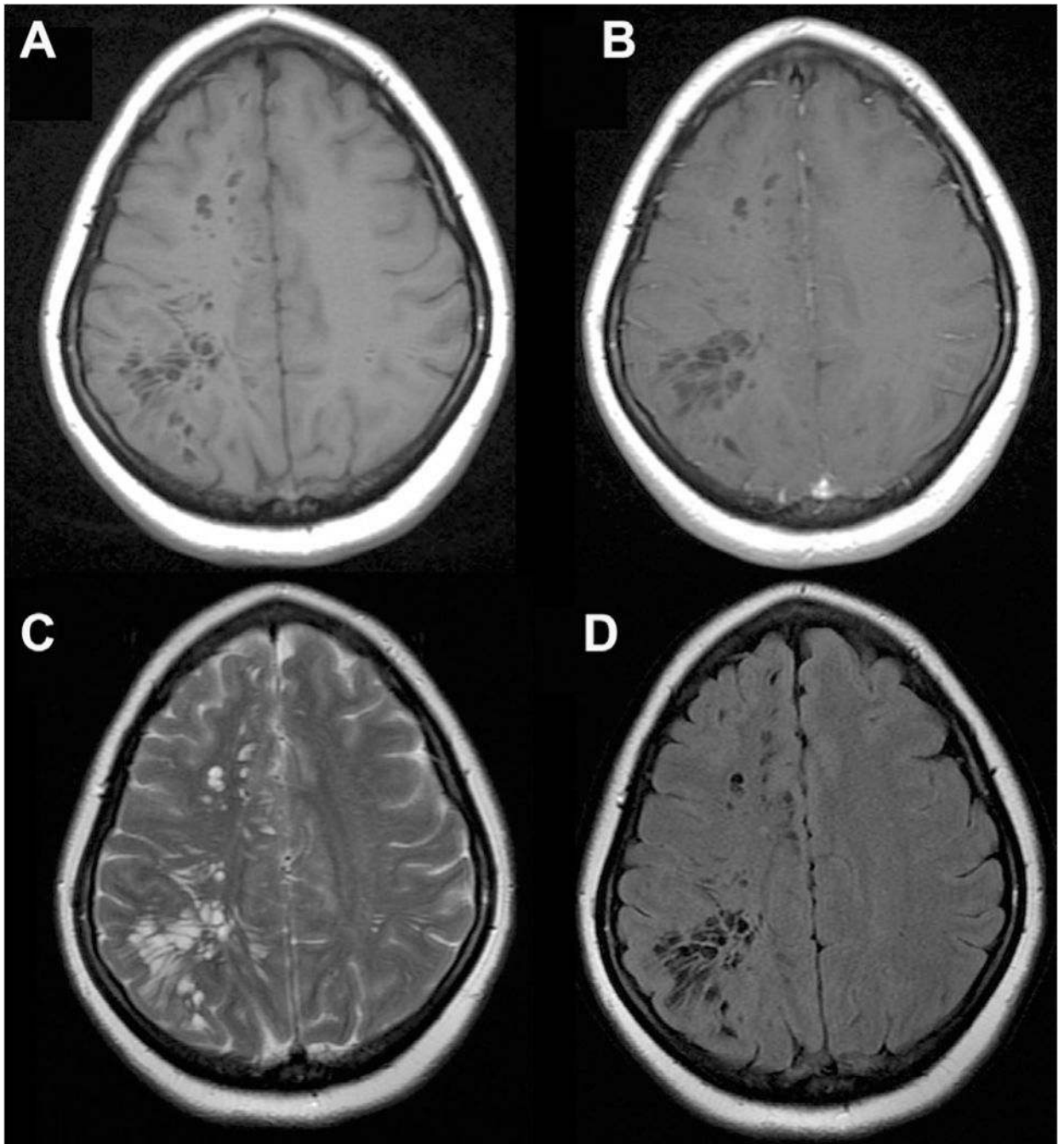


Fig 3. Sample-dilated PVSs in the superior right cerebral hemisphere subcortical white matter. The PVSs are isointense to CSF on T1 (A), T1 postcontrast (B), T2 (C), and FLAIR (D) axial MR images.

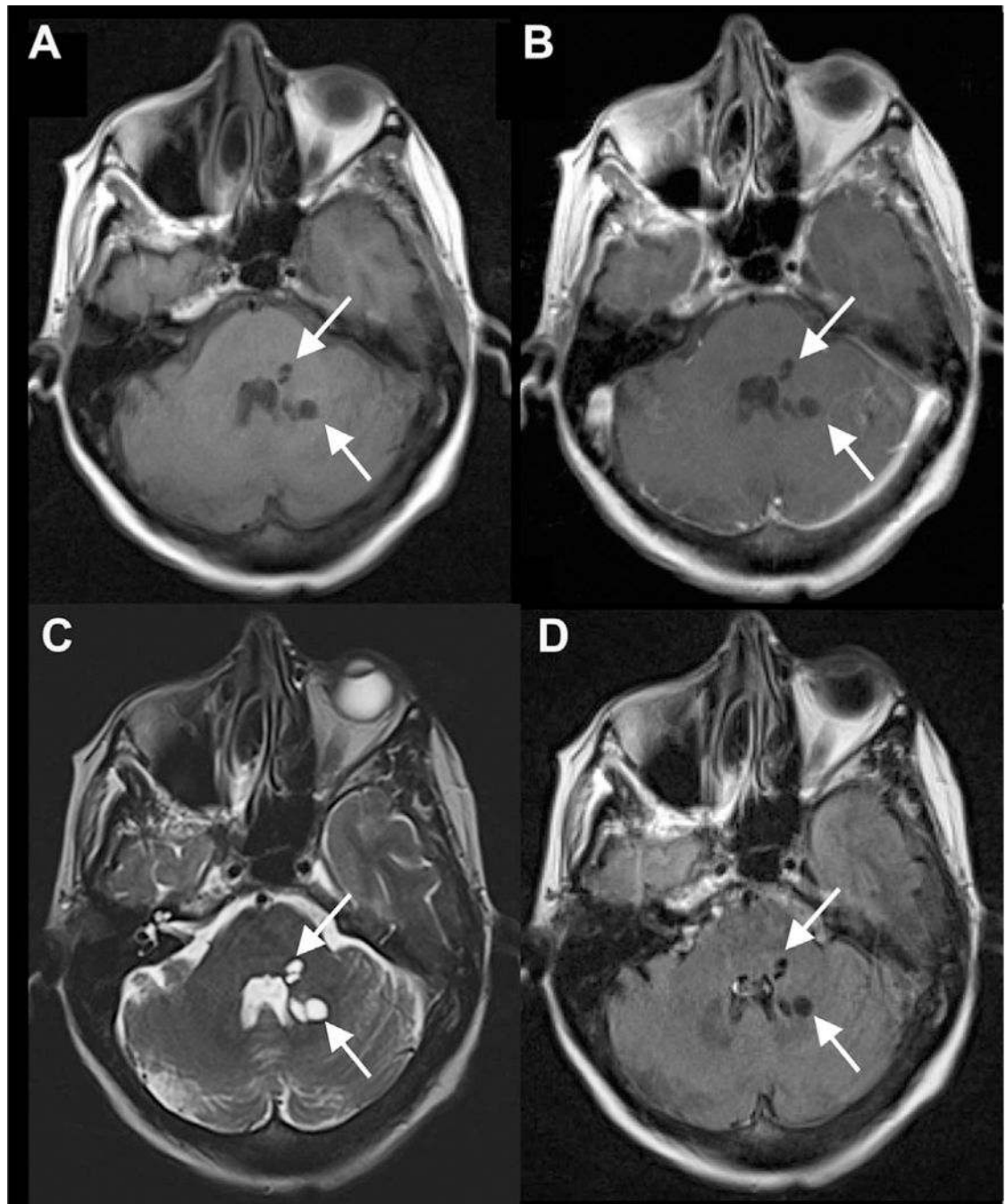


Fig 4. Dilated PVs in cerebellum. The PVs are isointense to CSF on T1 (A), T1 postcontrast (B), T2 (C), and FLAIR (D) axial MR images.

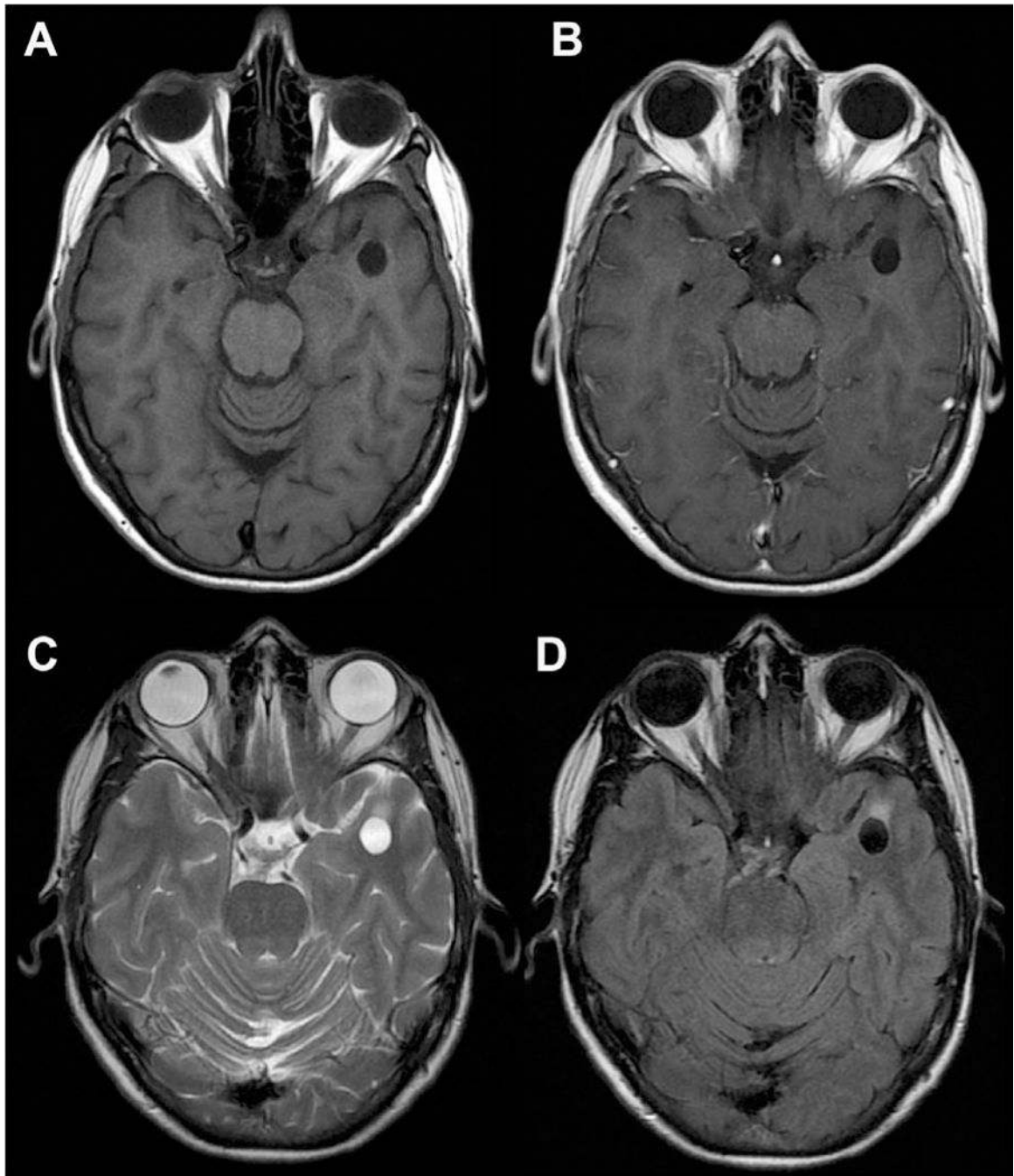


Fig 5. Dilated anterior temporal PVS. The perivascular space is isointense to CSF on T1 (A) and T1 postcontrast (B) MR images, but there is some mild associated T2/FLAIR signal abnormality (C, D), which is atypical for dilated PVS.

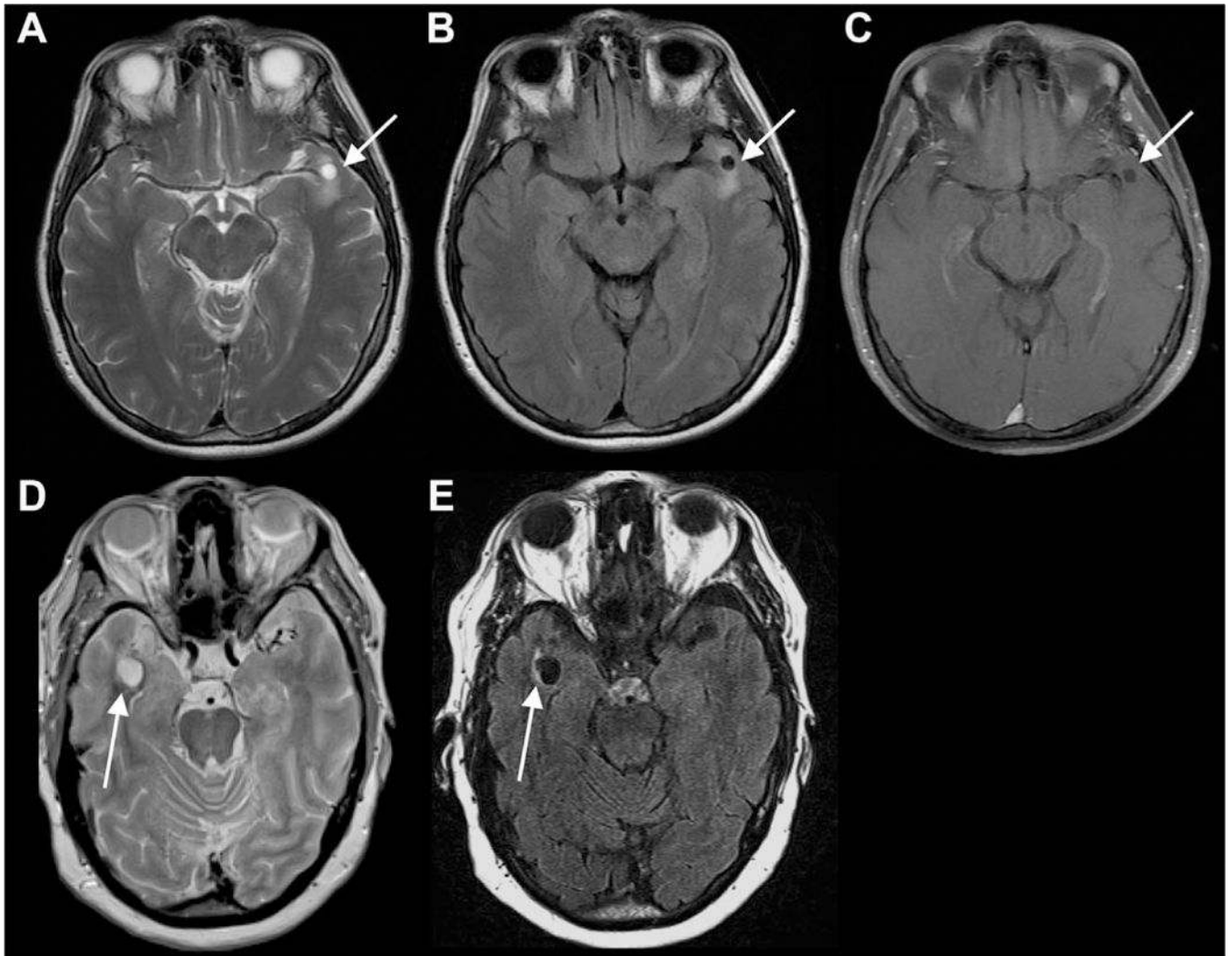


Fig 6. Additional sample-dilated anterior temporal PVSSs. The PVSSs are isointense to CSF on all sequences and do not exhibit contrast enhancement (C), but there is some mild associated T2/FLAIR signal abnormality (A, B, D, E), which is atypical for dilated a PVS.

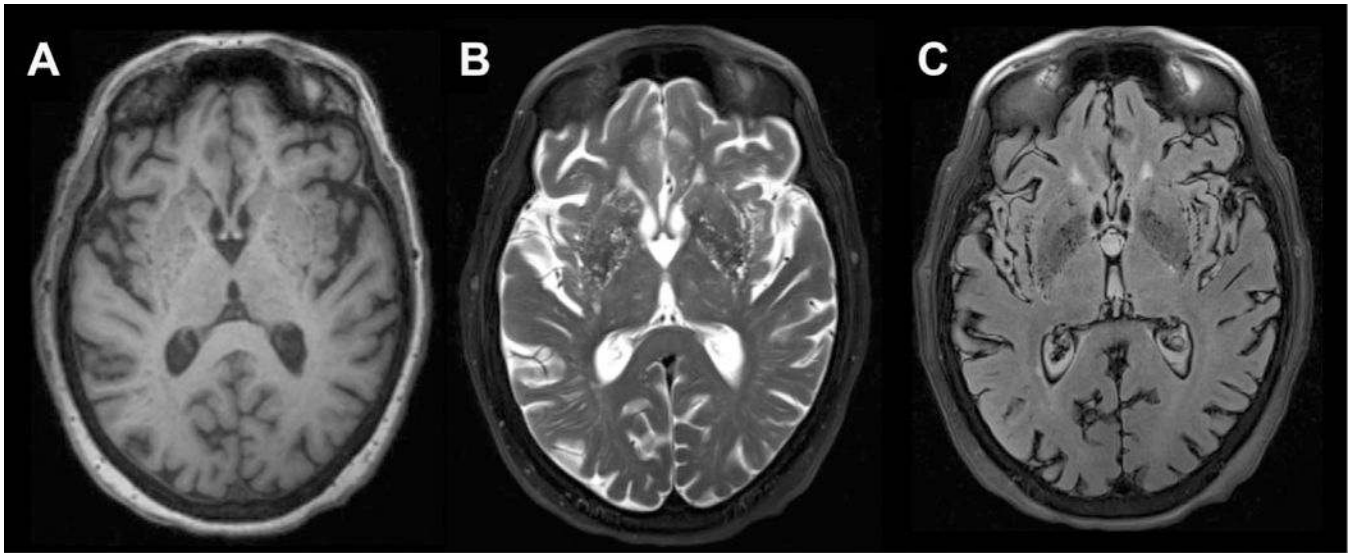


Fig 7. Patient with multiple prominent basal ganglia PVSs. The multiple PVSs are consistent with the described “état crible” pattern as seen on axial T1 (A), T2 (B), and FLAIR (C) MR images.

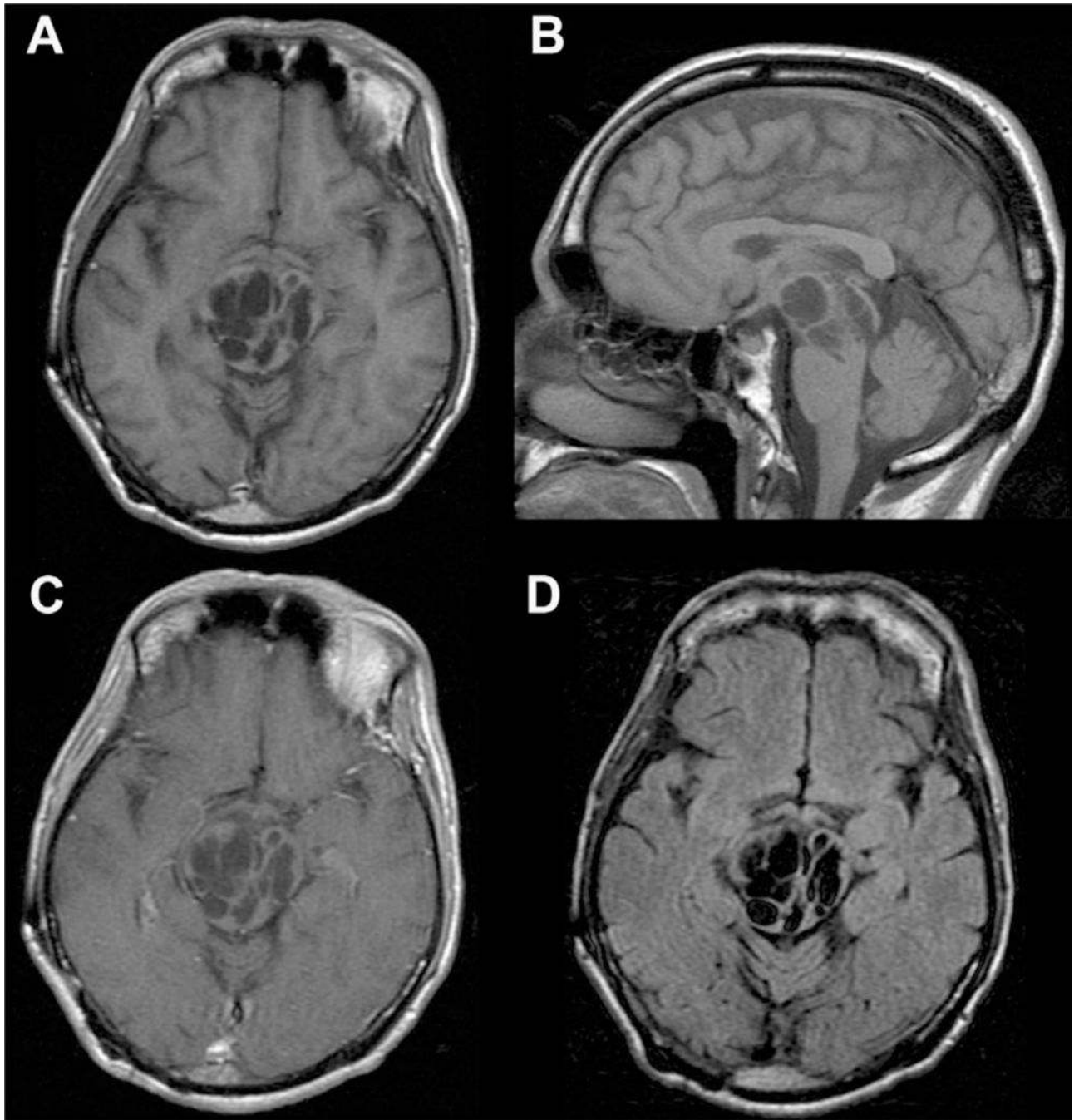


Fig 8. Giant/tumefactive PVSs. Multiple dilated cystic foci seen in the pons and midbrain extending into the right thalamus with CSF signal intensity consistent with a giant/tumefactive PVS as seen on axial and sagittal T1 (A, B), axial T1 postcontrast (C), and axial FLAIR (D) MR images.

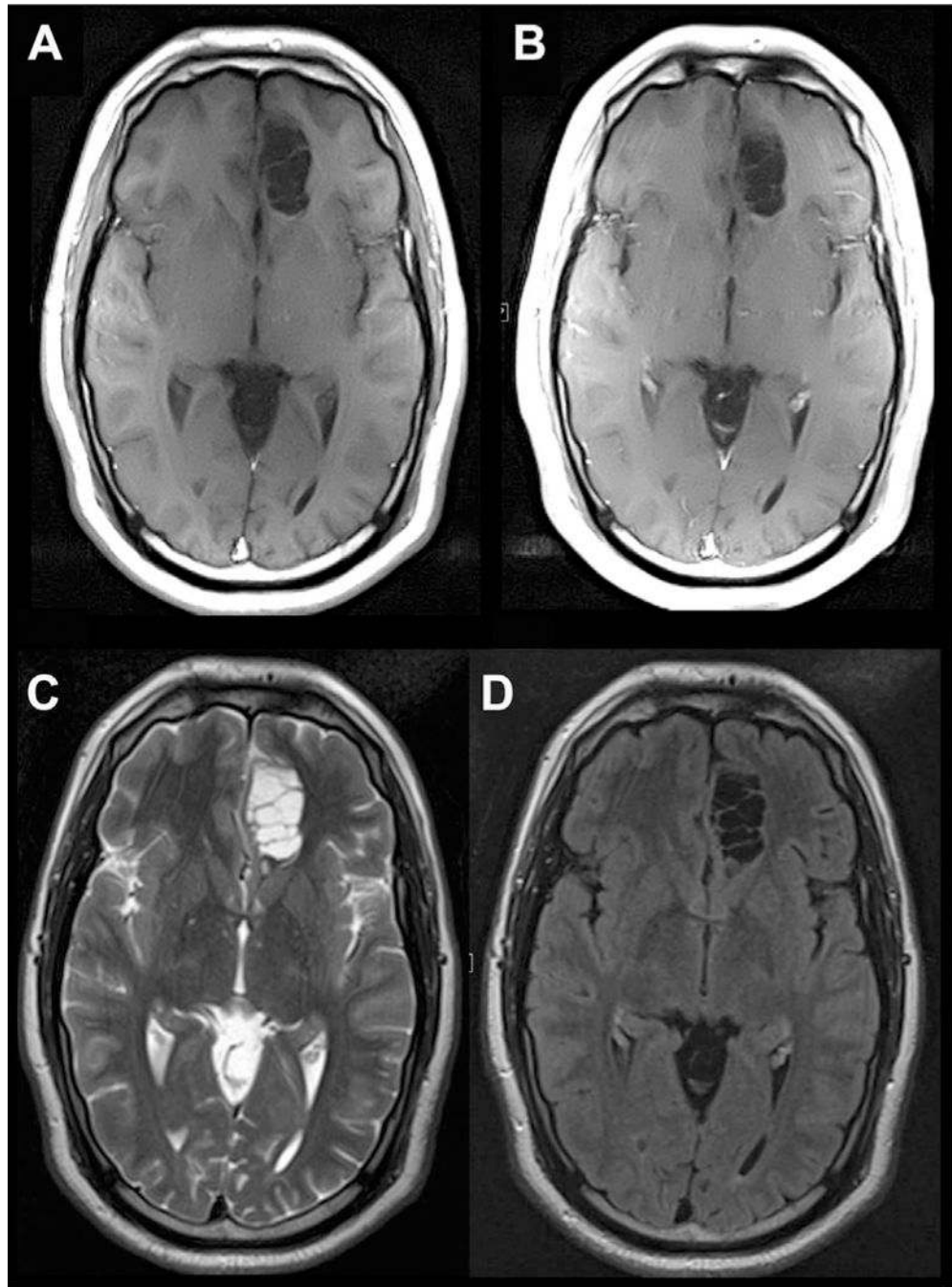


Fig 9. Giant/tumefactive PVSs in the left medial frontal lobe. The PVSs are isointense to CSF on T1 (A), T1-post contrast (B), T2 (C), and FLAIR (D) axial MR images.

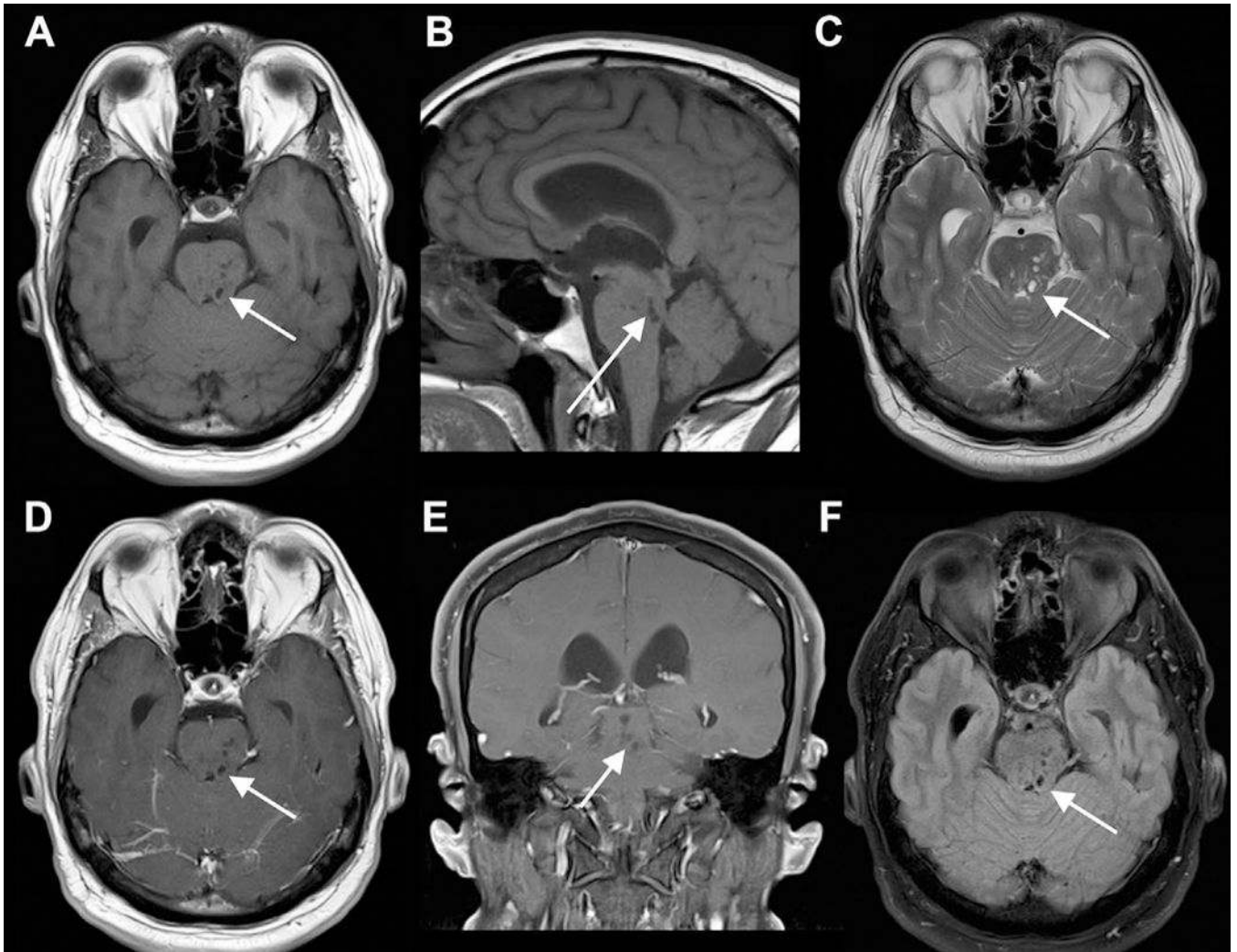


Fig 10. Minimally dilated PVS causing hydrocephalus. Small dilated PVSs in the midbrain (left more than right) and pons seen on axial and sagittal T1 (A, B), axial T2 (C), axial and coronal T1 postcontrast (D, E), and axial FLAIR (F) MR images. The PVSs are isointense to CSF on all sequences. The lateral and third ventricles are dilated, consistent with compensated, obstructive hydrocephalus.

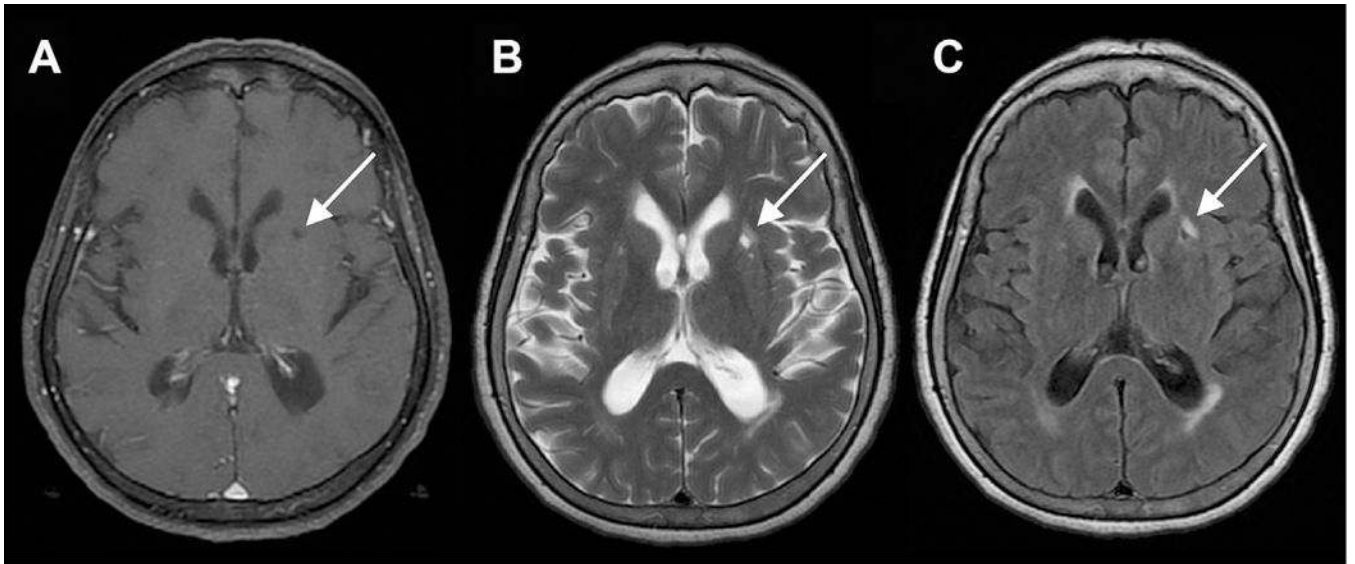


Fig 11. Left basal ganglia lacunar infarct. Four-millimeter ovoid lesion in the anterior left putamen with CSF signal centrally as seen on axial T1 (A), T2 (B), and FLAIR MR images. There is a surrounding rim of T2/FLAIR hyperintensity (B, C), typical of a chronic lacunar infarct.

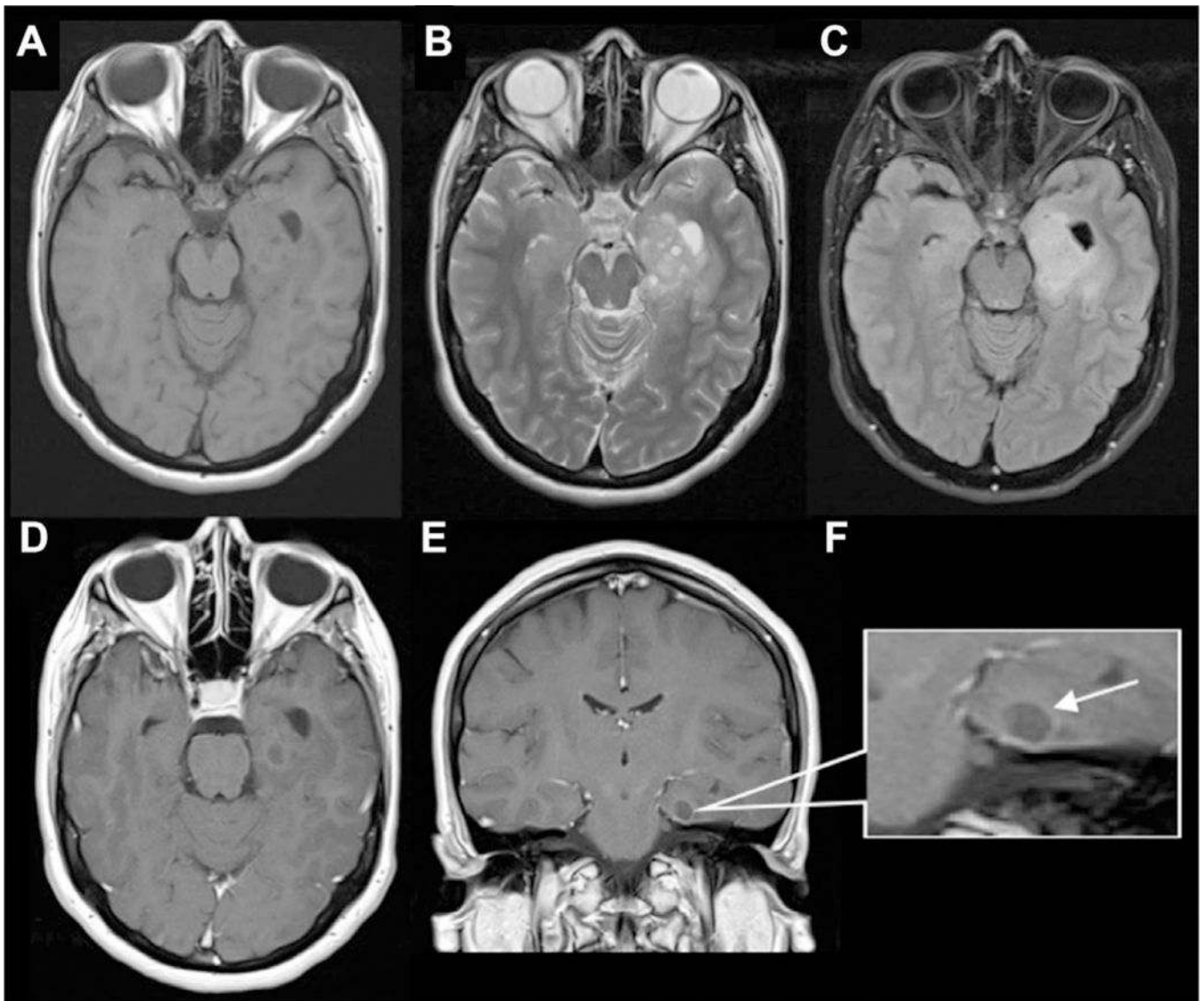


Fig 12. Dysembryoplastic neuroepithelial tumor (DNET) mimicking dilated PVS. There are numerous small- to medium-sized cystic lesions with “bubbly appearance” involving the amygdala, anterior hippocampus, and anterior parahippocampal gyrus are seen on (A) axial T1 (B) and axial T2 images. There is a larger area of surrounding expansile FLAIR signal abnormality (C) extending through the left posterior hippocampus, mid-fusiform gyrus, and temporal periventricular white matter along the inferolateral temporal horn. Faint peripheral enhancement around one of cystic components in the left parahippocampal gyrus on axial and coronal T1 postcontrast images (D, E).

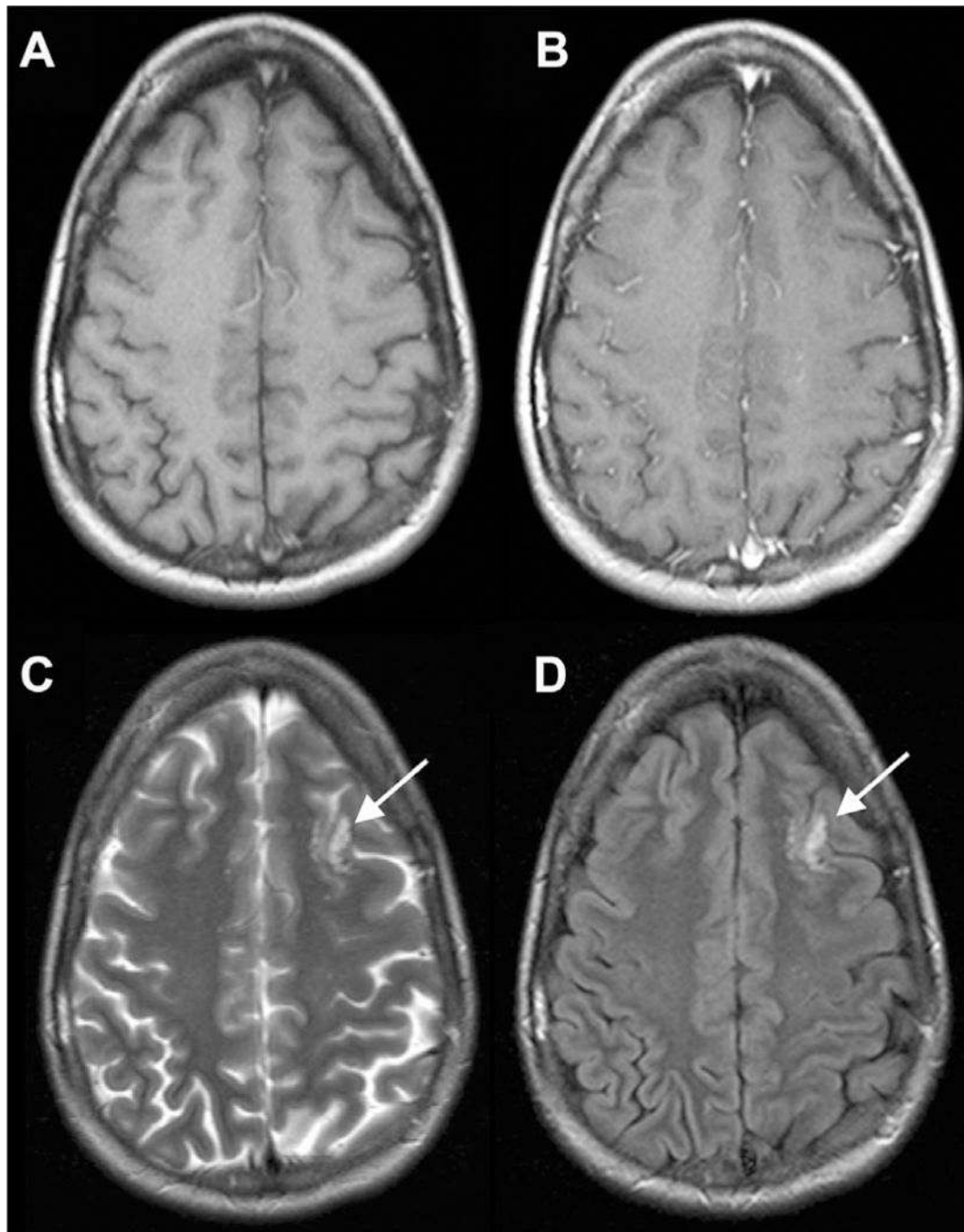


Fig 13. Multinodular and vacuolating neuronal tumor mimicking prominent PVS. There is a cluster of well-delineated, variable sized FLAIR/T2 hyperintense cysts (C, D) within the left frontal subcortical white matter, without obvious mass effect, or postcontrast enhancement on the T1 precontrast and T1 postcontrast MR images (A, B).

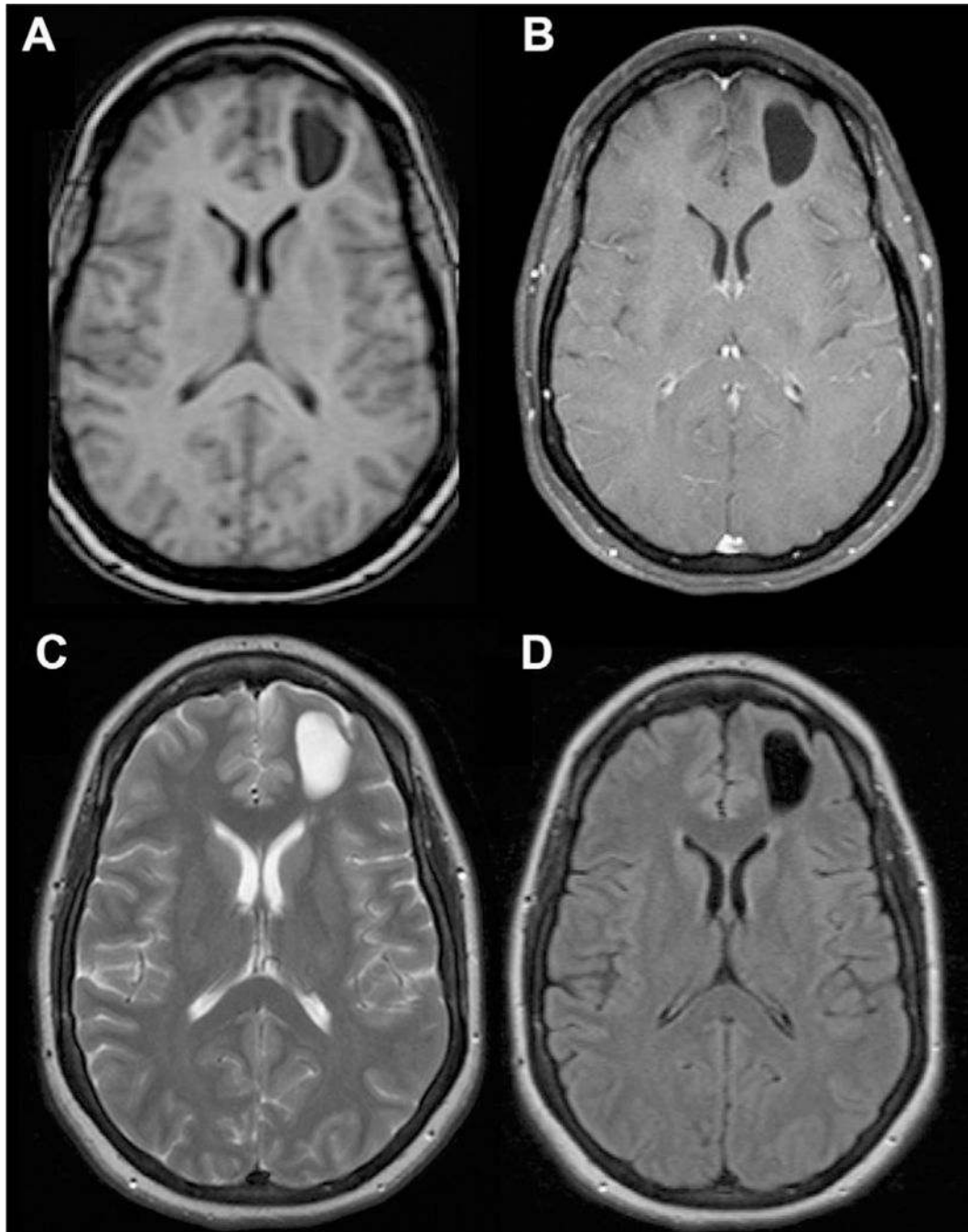


Fig 14. Intra-axial neuroglial cyst. CSF-filled lesion centered in the left frontal white matter without associated enhancement (A, B) or abnormal T2/FLAIR signal (C, D).

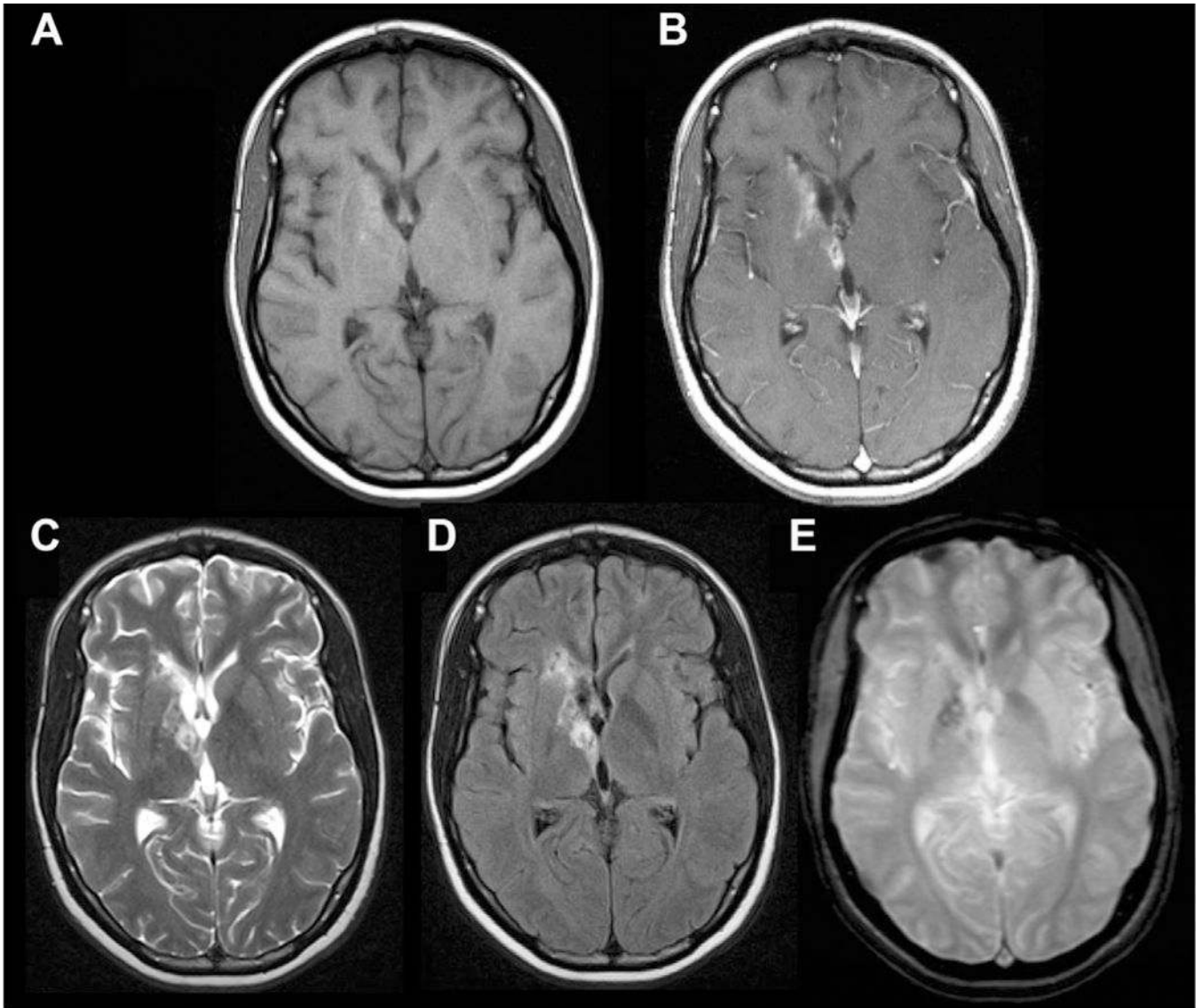


Fig 15. Case of neurotoxoplasmosis. Axial T1 pre- and postcontrast (A, B), T2 (C), FLAIR (D), and GRE (E) MR images. In the right basal ganglia, there are tiny cystic foci with surrounding intrinsic T1 shortening (A), T2/FLAIR hyperintensity (C, D), abnormal enhancement (B), and mild susceptibility (E).

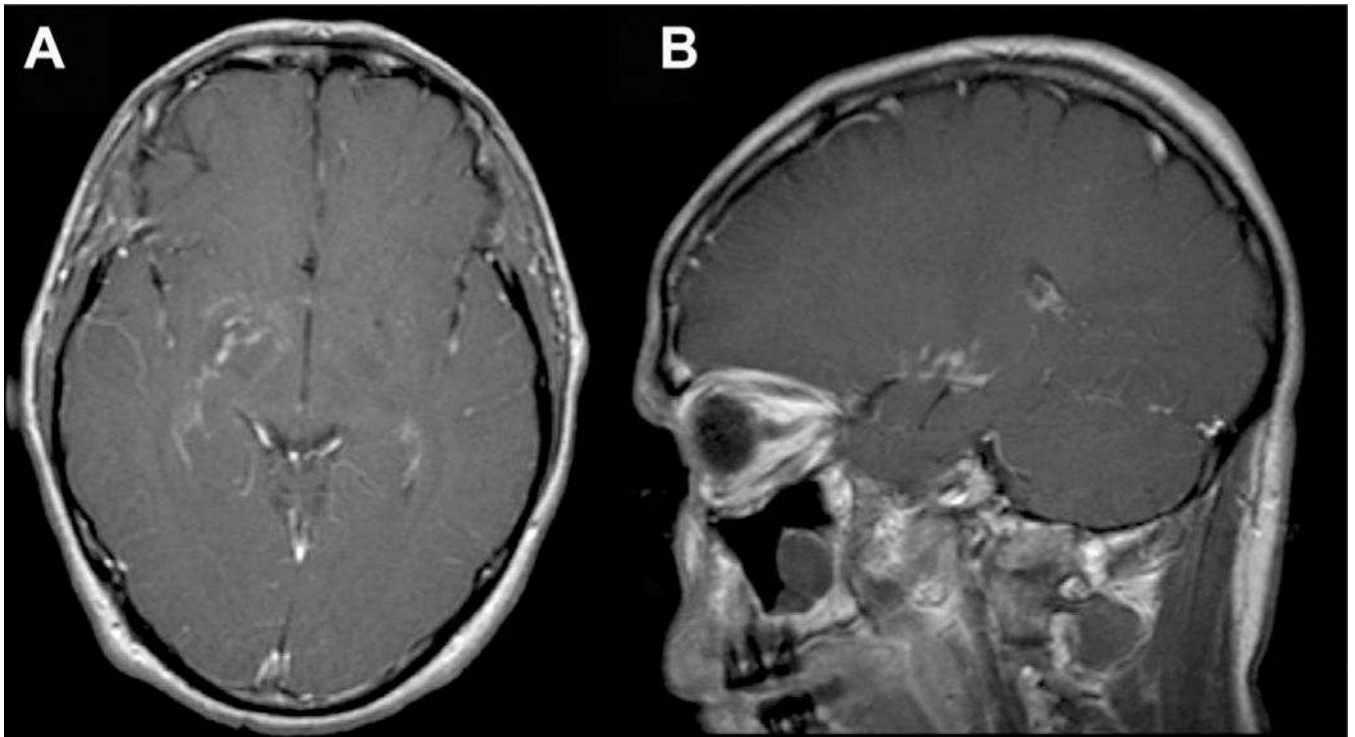


Fig 16. CNS cryptococcosis directly involving the PVS in a patient with human immunodeficiency virus. There is enhancement along the PVSs in the right greater than left basal ganglia seen on T1 postcontrast axial (A) and sagittal images (B).

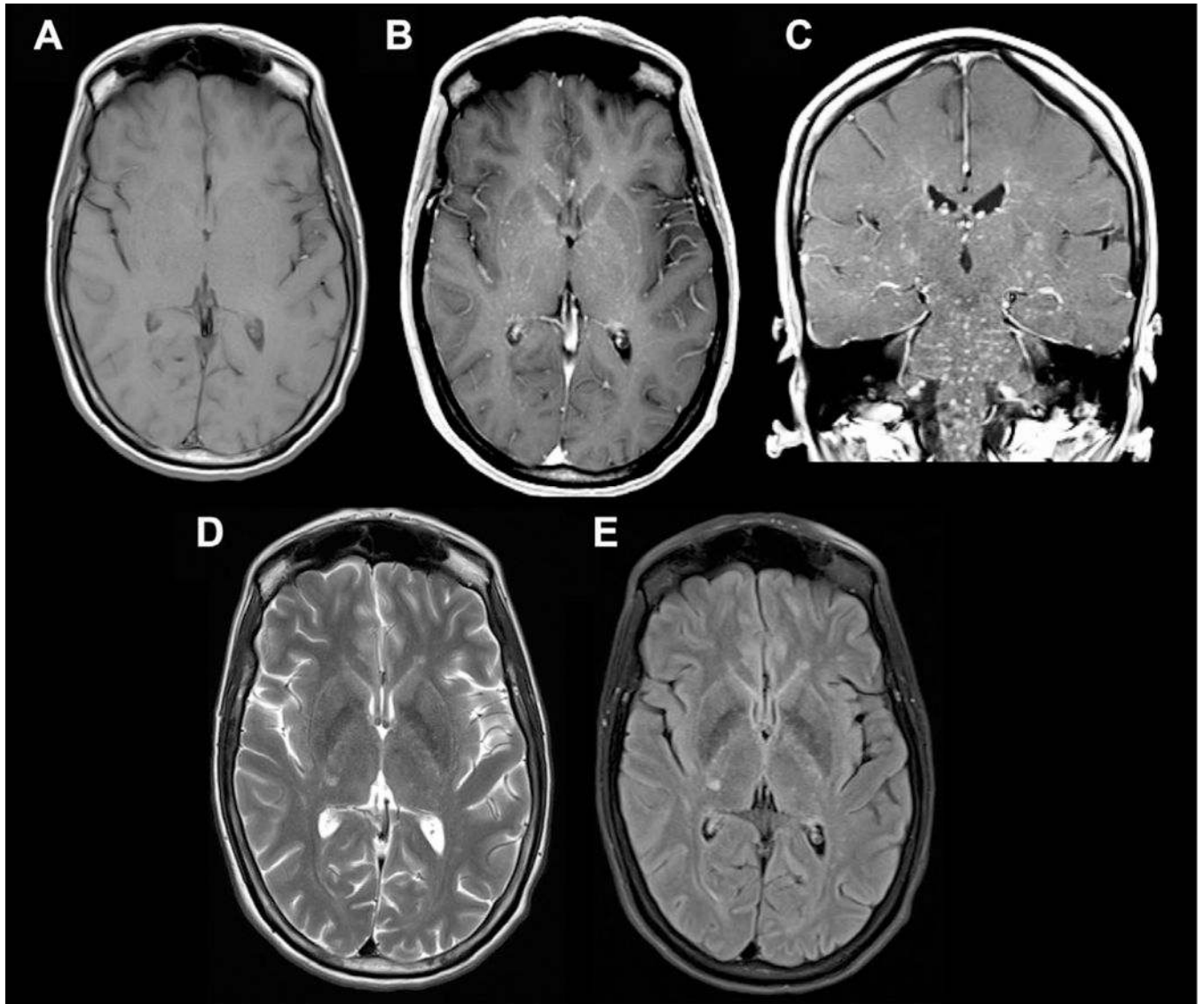


Fig 17. Sample case of intravascular neurosarcoidosis involving the PVSs. Axial T1 (A), axial and coronal T1 postcontrast (B, C), and axial T2/FLAIR images (D, E). There are innumerable punctate T2/FLAIR hyperintense enhancing nodules in the centrum semiovale, corona radiata, basal ganglia, brainstem, and visualized upper cervical spine bilaterally, which largely appear near the deep penetrating vessels along PVSs.

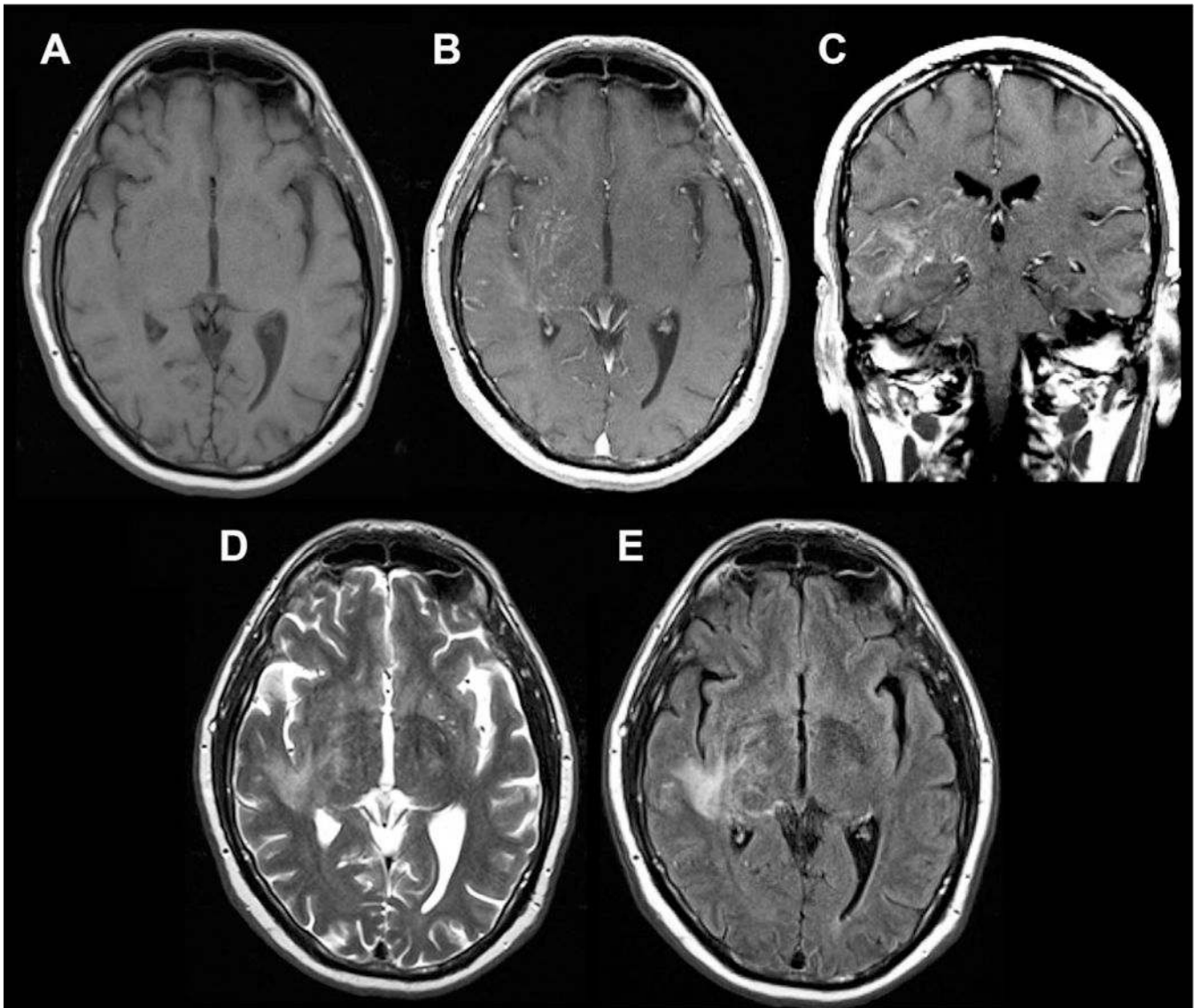


Fig 18. Sample case of intravascular CNS lymphoma involving PVSs, seen on axial T1 (A), axial and coronal T1 postcontrast (B, C), and axial T2/FLAIR images (D, E). There is linear, predominantly perivascular enhancement extending from the right thalamus and basal ganglia into the corona radiata, frontal, parietal, and temporal lobes with associated T2/FLAIR signal abnormality.

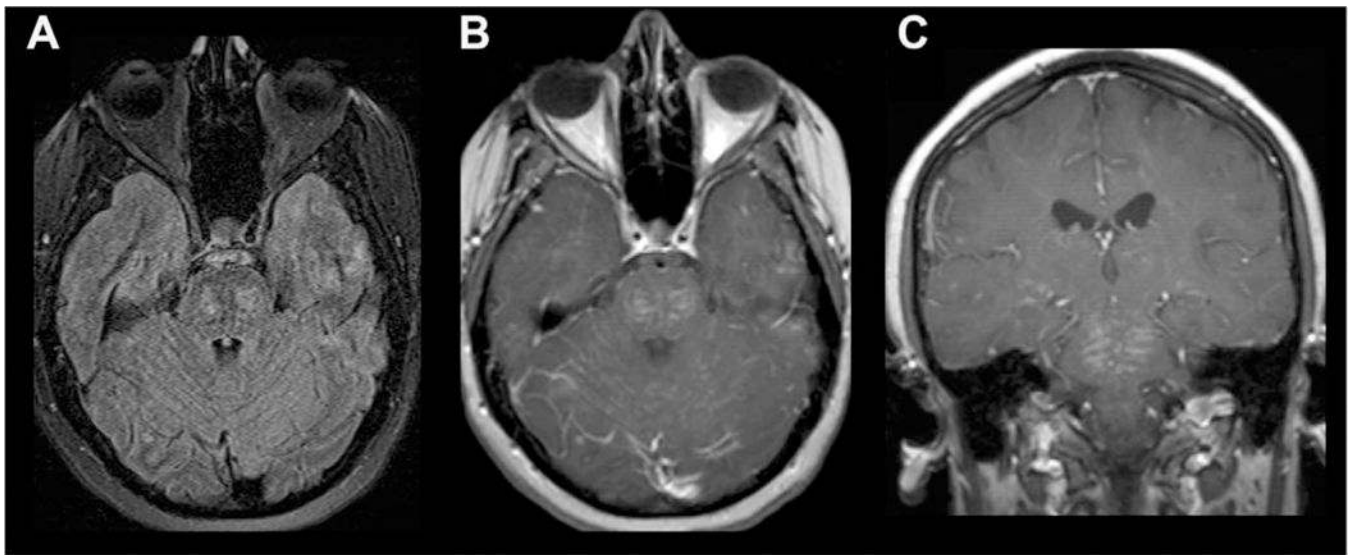


Fig 19. Chronic lymphocytic inflammation with pontine perivascular enhancement responsive to steroids (CLIPPERS) involving the PVSs. Diffuse leptomeningeal enhancement in the midbrain, pons, and medulla is seen on T1 postcontrast images (B, C) with foci of T2/FLAIR prolongation (A).

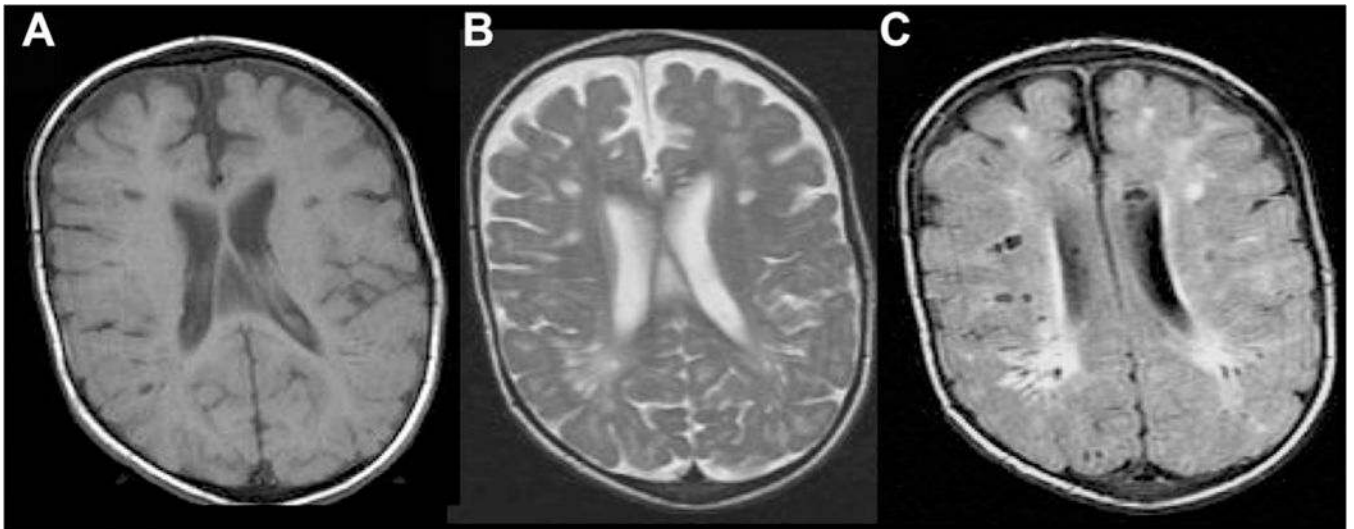


Fig 20. Sample case of mucopolysaccharidosis involving the PVSs reproduced from Mohan et al with permission. There are multiple bilateral cystic lesions (isointense to CSF on T1; A) in the subcortical white matter with associated surrounding T2/FLAIR hyperintensity (B, C).